Available online at www.sciencedirect.com
ScienceDirect
Journal of Power Sources 175 (2008) 183–188
JOURNAL OF POWER SOURCES
www.elsevier.com/locate/jpowsour

Short communication

A novel self-humidifying membrane electrode assembly with water transfer region for proton exchange membrane fuel cells

Er-Dong Wang, Peng-Fei Shi *, Chun-Yu Du

Department of Applied Chemistry, Harbin Institute of Technology, Harbin 150001, PR China

Received 17 September 2007; received in revised form 25 September 2007; accepted 25 September 2007
Available online 29 September 2007

Abstract

A novel self-humidifying membrane electrode assembly (MEA) with the active electrode region surrounded by a unactive "water transfer region (WTR)" was proposed to achieve effective water management and high performance for proton exchange membrane fuel cells (PEMFCs). By this configuration, excess water in the cathode was transferred to anode through Nafion membrane to humidify hydrogen. Polarization curves and power curves of conventional and the self-humidifying MEAs were compared. The self-humidifying MEA showed power density of 85 mW cm^{-2} at 0.5 V, which is two times higher than that of a conventional MEA with cathode open. The effects of anode hydrogen flow rates on the performance of the self-humidifying MEA were investigated and its best performance was obtained at a flow rate of 40 ml min^{-1}. Its performance was the best when the environmental temperature was 40 °C. The performance of the self-humidifying MEA was slightly affected by environmental humidity. The area of WTR was optimized, and feasible area ratio of the self-humidifying MEA was 28%.

Keywords: Proton exchange membrane fuel cell; Membrane electrode assembly; Self-humidifying; Water transfer region; Water management

1. Introduction

During the past two decades, the proton exchange membrane fuel cell (PEMFC) has been regarded as one of most promising alternative power sources, especially for portable applications, due to its high efficiency and low emission [1–5]. However, for commercial application as portable power sources, the structure of PEMFCs has to be designed as simply as possible to meet the weight and volume requirements [6–8]. Therefore, there is a urgent drive to remove the humidifier and heating device from the common PEMFC design. It is well known, however, that both the Nafion membrane and the Nafion electrolyte material in the catalyst layers need to be hydrated in order to conduct proton efficiently [9,10]. In addition, excess water produced in the cathode catalyst layer has to be removed to avoid cathode "flooding", especially at low temperature. Thus, removement of humidifier and heating device from the PEMFC will result in severe water management issues. A self-humidifying system, which humidifies the anode side of the Nafion membrane and removes the liquid water at the cathode efficiently, is strongly required.

A lot of efforts have been made for self-humidifying PEMFCs. Most of the ideas were focused on the fabrication of self-humidifying membranes by incorporating highly dispersed nano-size Pt particles in the Nafion membrane [11–14]. By this way, Pt nanoparticles were expected to catalyze the recombination of H_2 and O_2 diffusing into the Nafion membrane, which, on the one hand, decreased the reactants crossover through Nafion membrane, and on the other hand, increased the water content in the Nafion membrane, reducing the proton transport resistance. This method, however, had some disadvantages, including high cost and formation of an electron-conducting path via the network of dispersed Pt or Pt/C particles [15]. To avoid the possibility of a short circuit through the membrane, some double-layer or sandwich type composite membranes were proposed [16,17]. In addition, to replace Pt particles, some hydrophilic inorganic oxides were added into the Nafion membrane or the anode catalyst layer in order to increase the

* Corresponding author. Tel.: +86 451 86413721; fax: +86 451 86413720.
E-mail address: pfshi@hit.edu.cn (P.-F. Shi).

0378-7753/$ – see front matter © 2007 Elsevier B.V. All rights reserved.
doi:10.1016/j.jpowsour.2007.09.075

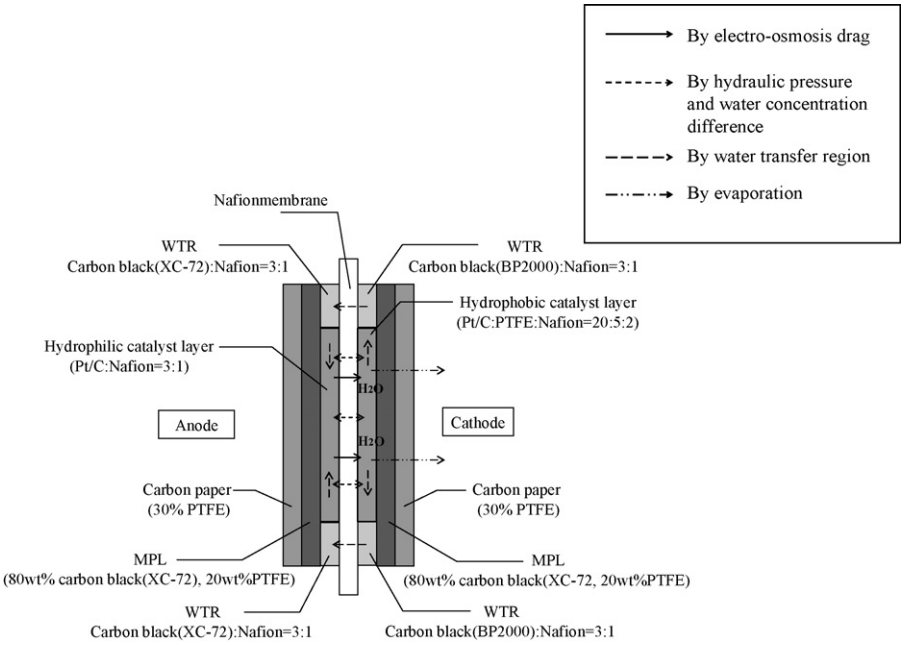

Fig. 1. Section structure of the self-humidifying MEA and water transfer route in the self-humidifying MEA.

uptake of water inside the Nafion membrane or the anode catalyst layer [18–21]. Nevertheless, no matter what kind of particles was added in the membrane or the anode catalyst layer, the water content in the anode was still difficult to be maintained, due to the electro-osmotic drag of water from the anode to the cathode. More importantly, this method contributed little to the water removal in the cathode, which was very important to the PEMFC performance, especially at high current densities. Some studies have been undertaken to address both the anode humidification and the cathode water removal. Ge et al. used a water-absorbing sponge made of polyvinyl alcohol to develop an internally humidified system. The water-absorbing sponge was advantageous for humidification of the dry inlet air and for removal of liquid water from the cell [22]. Williams et al. modified the gas diffusion layer by coating carbon black and 14 wt.% PTFE onto the macro-porous substrate using a silk-screen technique, and improved cell performance under low and no external humidification conditions [23].

In this study, a novel self-humidifying MEA with the active electrode region (AER) surrounded by water transfer region (WTR) for PEMFCs was presented as shown in Fig. 1. In this configuration, excess water at the cathode was expected to transfer to the cathode WTR, which significantly reduced the water flooding. The water in the cathode WTR then diffuses through the Nafion membrane to the anode WTR, and finally transfers to the strongly hydrophilic active anode region, which hydrates the anode side of the membrane, and thus reduces the ohmic polarization of the MEA significantly. The performances of both our self-humidifying MEA and the conventional MEA were firstly compared by the polarization and power curves. The effects of the hydrogen flow rate and environmental conditions on the performance of the self-humidifying MEA were then investigated. Finally, the area of WTR was optimized and the self-humidifying MEA with proper WTR area was chosen for PEMFC stacks.

2. Experimental

Nafion 112 membrane (DuPont) was used in our experiments and firstly boiled in 5 wt.% H_2O_2 solution for 1 h in order to remove organic and inorganic contaminants. After washing the membrane in deionized water for several times, the membrane was boiled in 0.5 mol l^{-1} H_2SO_4 solution for 2 h to convert the membrane into H^+ form. The membrane was then washed using deionized water repeatedly and stored in pure water for use.

Both the anode and cathode gas diffusion layers (GDL) consisted of 30 wt.% PTFE bonded carbon paper (TGP-H-090, Toray) as backing layer and 20 wt.% PTFE contained carbon black (XC-72, Cabot) as microporous layer (MPL). Before brushing the catalyst layer onto the GDL, the mixture of carbon black and Nafion (3:1 w/w) was sprayed onto the peripheral region, i.e., the WTR, of the catalyst layer. The catalyst layer was then obtained by brushing the catalyst slurry onto the central area of the GDL. The self-humidifying MEA was finally obtained by hot-pressing the Nafion membrane, the anode, and the cathode at 135 °C with a pressure of 1.8 MPa for 2 min. For the cathode, BP2000 carbon black with 1.5 mg cm^{-2} loading was for the WTR, and 20 wt.% Pt/C (E-TEK), PTFE and Nafion (20:5:2) with 0.3 mg cm^{-2} Pt loading were for the catalyst layer. For the anode, the XC-72 carbon black with 1.0 mg cm^{-2} loading was for the WTR, and 20 wt.% Pt/C and Nafion (3:1,) with Pt loading of 0.2 mg cm^{-2} was for the catalyst layer. The main consideration for the composition difference between the anode and the cathode is to eject water from cathode catalyst layer and maintain water in anode catalyst layer. For comparison, the conventional MEA without the WTR was prepared using the

Table 1
Abbreviations and sizes of the self-humidifying MEAs and conventional MEA

	MEA sample			
	NOV 1	NOV 2	NOV 3	CON
Size	2 cm × 5 cm	1.6 cm × 4.6 cm	1.3 cm × 4.3 cm	1 cm × 4 cm
Area of WTR	6 cm^2	3.36 cm^2	1.59 cm^2	–
Area ratio of WTR	60%	45.7%	28.4%	–

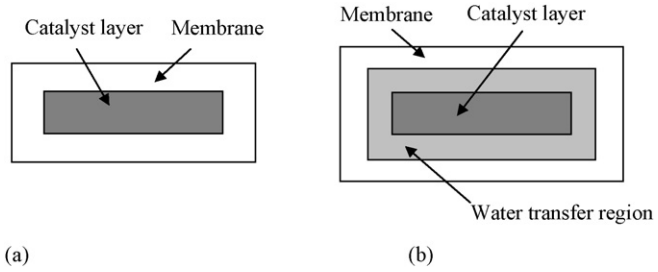

Fig. 2. Structures of conventional MEA and the self-humidifying MEA.

similar method and materials with the self-humidifying MEA. The active electrode areas for the self-humidifying MEAs and the conventional MEA were all 1 cm × 4 cm. The abbreviations and sizes of self-humidifying MEAs and conventional MEA were shown in Table 1.

Both the novel self-humidifying and conventional MEAs, schematically presented in Fig. 2, were assembled into single cells and tested using Neware Cell Test equipment (ShenZhen, China). The cells were operated in a sealed operation box, where the environmental temperature was controlled by a heating plate and the environmental humidity was adjusted by a mini-type humidifier. Dry hydrogen was used as the anode fuel, and dry oxygen or air were fed as cathode oxidants.

3. Results and discussion

3.1. Performance comparison of the self-humidifying MEA and the conventional MEA

The comparison of performance curves for the conventional and the self-humidifying MEAs are presented in Figs. 3 and 4. Inspiringly, the performance of the self-humidifying MEA is markedly higher than that of the conventional one, especially at high current densities. This performance improvement of the self-humidifying MEA should be attributed to presence of the WTR, because the WTR was the only difference for the two kinds of MEAs. For the conventional MEA, water loss at the anode, resulted from the electro-osmotic drag, could cause the anode drying and increase the membrane resistance severely. In addition, water in the cathode catalyst layer could not be ejected efficiently, and thus, water flooding and concentration polarization appeared, especially for air as oxidant. In contrast to the case of the conventional MEA, for the novel self-humidifying MEA, on the one hand, excess water at the cathode could be conveniently transferred to the cathode WTR, which significantly reduced water flooding and concentration polarization of oxygen; on the other hand, water in the cathode WTR could diffuse through the Nafion membrane to the anode WTR, and then transferred to the anode catalyst layer because the anode catalyst layer was highly hydrophilic, which hydrated the membrane and reduced the ohmic polarization of the MEA significantly. At high current densities, water flooding at the cathode and the membrane drying at the anode were more severe, and thus, the self-humidifying MEA showed much better cell performance by the more efficient water management.

3.2. Effect of hydrogen flow rate on the self-humidifying MEA

To optimize the performance of the self-humidifying MEA, effects of some operation conditions on the cell performance were investigated. The effect of the anode hydrogen flow rate on the self-humidifying MEA was illustrated in Fig. 5. At low and medium current densities, the performance of the self-

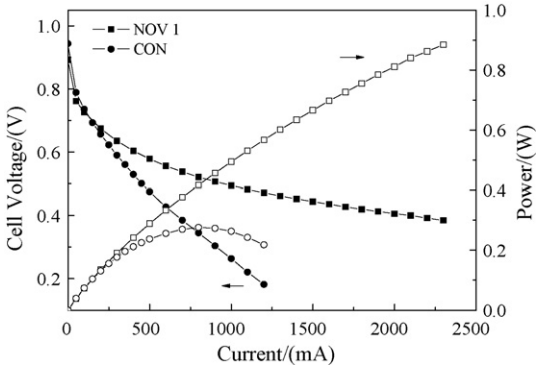

Fig. 3. Polarization curves and power curves of the self-humidifying and conventional MEA in oxygen at 20 °C.

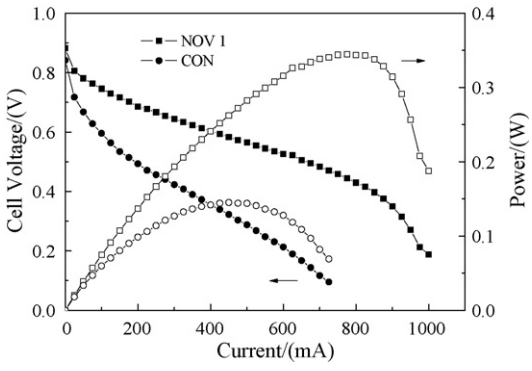

Fig. 4. Polarization curves and power curves of the self-humidifying and conventional MEA in air with cathode open at 20 °C.

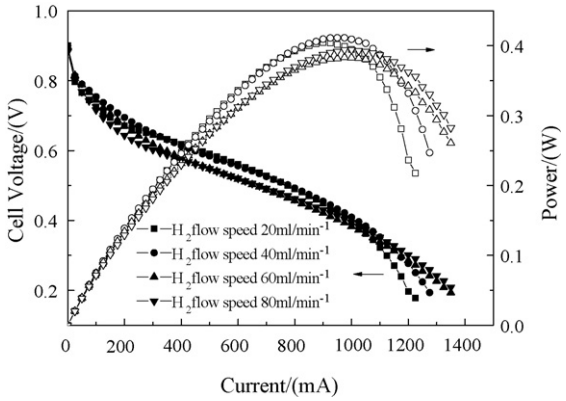

Fig. 5. The effect of different hydrogen flow rates on the self-humidifying MEA with cathode open at 20 °C.

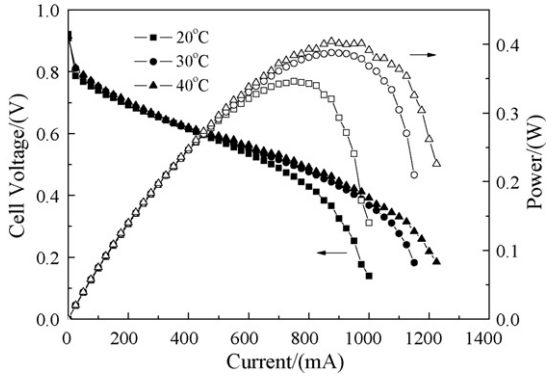

Fig. 7. The effect of different environmental temperature on the self-humidifying MEA with cathode open.

humidifying MEA for low hydrogen flow rates was better than that for high hydrogen flow rates. At high current densities, however, the self-humidifying MEA for high hydrogen flow rates presented better performance. This observation could be explained as follows. At low and medium current densities, where the ohmic polarization was dominant, the better performance of the self-humidifying MEA for low hydrogen flow rates could be attributed to the lower membrane resistance, which resulted from the less anode water loss taken away by the lower hydrogen flow rate. At high current densities, where the concentration polarization was dominant, the better performance of the self-humidifying MEA for higher hydrogen flow rates could not be attributed to the improvement of the hydrogen transport, because it was calculated that the theoretically required hydrogen flow rate was significantly lower than 20 ml min^{-1} and thus the limitation of hydrogen transport could be excluded. Therefore, this performance improvement could only be attributed to the oxygen transport limitation. When the cell was operated at high current densities, large amount of water was produced at the cathode catalyst layer, causing the cathode flooding. High hydrogen flow rate at the anode could take away more anode water, which increased the concentration gradient of water, and thus, the water diffusion rate from the cathode to the anode was increased. Therefore, water flooding at the cathode could be reduced and oxygen could diffuse to the cathode catalyst layer more easily. After the polarization test, liquid water accumulated at the open cathode with different hydrogen flow rates was recorded, as illustrated in Fig. 6. Clearly, liquid water at the cathode was decreased with the increase in the anode hydrogen flow rate, and there was almost no liquid water existed on the surface of the cathode at the hydrogen flow rate of 80 ml min^{-1}, which confirmed our explanation for the performance difference at high current densities. To obtain the maximum power performance for the self-humidifying MEA, the hydrogen flow rate of 40 ml min^{-1} was employed in the next experiments.

3.3. Effect of environmental temperature and humidity

Effects of the environmental temperature and humidity on the performance of the self-humidifying MEA were also investigated. Fig. 7 gives the effect of environmental temperature on the self-humidifying MEA. The performance of the self-humidifying MEA was greatly improved with increasing the environmental temperature, which could be ascribed to the more facile reaction kinetics, mass transport and proton transfer through Nafion membrane at higher temperatures. It was noteworthy that the performance improvement from 30 °C to 40 °C was less pronounced than that from 20 °C to 30 °C, indicating that the temperature effect was somewhat depressed at higher temperatures and that it was unnecessary to operate the self-humidifying MEA at too high temperature to achieve the best performance.

Fig. 8 shows the cell performance of the self-humidifying MEA for different environmental humidity. At low and medium current densities where ohmic polarization was dominant,

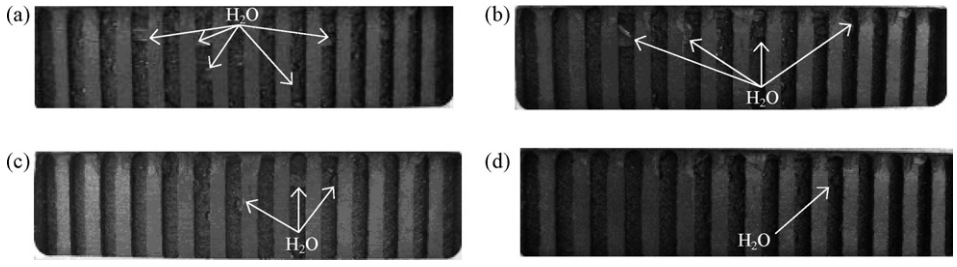

Fig. 6. State of water accumulation at open cathode with different hydrogen flow rates after polarization curves test: (a) 20 ml min^{-1}, (b) 40 ml min^{-1}, (c) 60 ml min^{-1}, and (d) 80 ml min^{-1}.

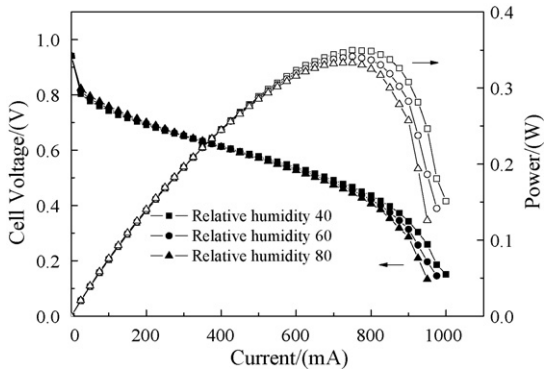

Fig. 8. The effect of different environmental humidity on the self-humidifying MEA with cathode open at 20 °C.

no visible performance difference was observed for different environmental humidity. At high current densities where concentration polarization was dominant, the performance of the self-humidifying MEA decreased with increasing of the environmental humidity, probably due to the fact that at higher environmental humidity, on the one hand, more liquid water at the cathode was condensed, which increased the oxygen transport resistance, and on the other hand, the oxygen mole fraction decrease, which also decrease the performance. Although the difference resulting from environmental humidity was existed, it was possibly reduced due to excellent water transfer ability from the cathode to the anode for the self-humidifying MEA.

3.4. Optimization of WTR area

In order to optimize the WTR area, three self-humidifying MEAs with different WTR areas, listed in Table 1, were prepared and tested. Fig. 9 shows the polarization curves for the three self-humidifying MEAs. No obvious performance difference between NOV 1 and NOV 2 MEAs was observed, and the performance of NOV 3 MEA was slightly lower than that of NOV 1 and NOV 2 MEAs. The results shows that water transfer ability will be reduced when the area ratio of WTR is about lower than 30%, which reduced in the decrease of cell performance.

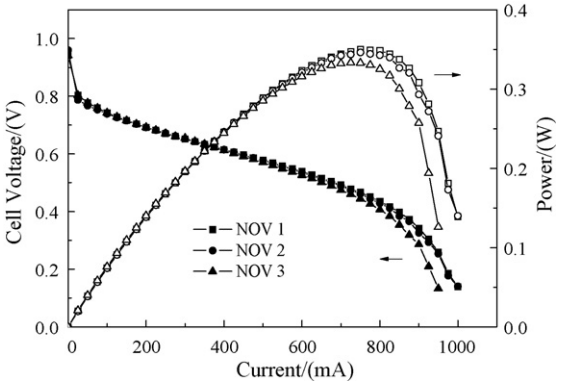

Fig. 9. Polarization curves and power curves of the self-humidifying MEAs with different WTR area with cathode open at 20 °C.

Mainly considering the size and cost of the self-humidifying MEAs, NOV 3 MEA with lowest WTR area was preliminarily chosen as the preferred self-humidifying MEA design in our next experiments. Further investigation and optimization of the WTR area by numerical simulation methods are on-going and the results will be presented later.

4. Conclusions

A novel self-humidifying MEA with WTR was prepared and evaluated. Compared with the conventional MEA, our self-humidifying MEA can improve the cell performance significantly. The self-humidifying MEA showed power density of 85 mW cm^{-2} at 0.5 V, which is two times higher than a conventional MEA. The performance of self-humidifying MEA was affected by different anode hydrogen flow rates, and the best performance was obtained at a flow rate of 40 ml min^{-1}. Cell performance was relatively good under higher environmental temperature. Cell voltage is slightly decreased as the environmental humidity is increased. The results showed that NOV 3 with the WTR area ratio of 28% was the best for practical application. Performance of the novel self-humidifying MEA was improved obviously without increasing the area of catalyst layer or the loading of catalyst. This novel structure can be a new attempt for the fabrication of self-humidifying MEA for PEMFC applications.

Acknowledgements

This work was supported by Coslight storage battery Co. Ltd. The author thanks Dr. Zhenbo Wang for his kindly help in the experiment and paper preparation.

References

[1] J. Larminie, A. Dicks, Fuel Cell Systems Explained, Wiley, Great Britain, 2000.
[2] P. Costamagna, S. Srinivasan, J. Power Sources 102 (2001) 242.
[3] P. Costamagna, S. Srinivasan, J. Power Sources 102 (2001) 253.
[4] R. Beneito, J. Vilaplana, S. Gisbert, Int. J. Hydrogen Energy 32 (2007) 1554.
[5] J.J. Hwang, D.Y. Wang, N.C. Shih, D.Y. Lai, C.K. Chen, J. Power Sources 133 (2004) 223.
[6] A.P. Vega-Leal, F.R. Palomo, F. Barragán, C. García, J. Javier Brey, J. Power Sources 169 (2007) 194.
[7] M. Oszcipok, M. Zedda, J. Hesselmann, M. Huppmann, M. Wodrich, M. Junghardt, C. Hebling, J. Power Sources 157 (2006) 666.
[8] K. Tüber, M. Zobel, H. Schmidt, C. Hebling, J. Power Sources 122 (2003) 1.
[9] S. Gottesfeld, Adv. Electrochem. Sci. Eng. 5 (1997) 195.
[10] M. Han, S.H. Chan, S.P. Jiang, Int. J. Hydrogen Energy 32 (2007) 385.
[11] M. Watanabe, H. Uchida, Y. Seki, M. Emori, J. Electrochem. Soc. 143 (1996) 3847.
[12] F.Q. Liu, B.L. Yi, D.M. Xing, J.R. Yu, Z.J. Hou, Y.Z. Fu, J. Power Sources 124 (2003) 81.
[13] D.H. Son, R.K. Sharma, Y.G. Shul, H.S. Kim, J. Power Sources 165 (2007) 733.
[14] H.K. Lee, J.I. Kim, J.H. Park, T.H. Lee, Electrochim. Acta 50 (2004) 761.

[15] T.H. Yang, Y.G. Yoon, C.S. Kim, S.H. Kwak, K.H. Yoon, J. Power Sources 106 (2002) 328.
[16] B. Yang, Y.Z. Fu, A. Manthiram, J. Power Sources 139 (2005) 170.
[17] Y.H. Liu, B.L. Yi, Z.G. Shao, L. Wang, D.M. Xing, H.M. Zhang, J. Power Sources 163 (2007) 807.
[18] A. Saccà, A. Carbone, E. Passalacqua, A. D'Epifanio, S. Licoccia, E. Traversa, E. Sala, F. Traini, R. Ornelas, J. Power Sources 152 (2005) 16.
[19] P.L. Antonucci, A.S. Arico, P. Creti, E. Ramunni, V. Antonucci, Solid State Ionics 125 (1999) 431.
[20] K.T. Adjemian, S. Srinivasan, J. Benziger, A.B. Bocarsly, J. Power Sources 109 (2002) 356.
[21] U.H. Jung, K.T. Park, E.H. Park, S.H. Kim, J. Power Sources 159 (2006) 529.
[22] S. Ge, X. Li, I.M. Hsing, Electrochim. Acta 50 (2005) 1909.
[23] M.V. Williams, H.R. Kunz, J.M. Fenton, J. Power Sources 135 (2004) 122.